Numerical Study of Nonstationary Phenomena in Gyro-Oscillators

OUTLINE

- Introduction
- Theory
  - Eigenfunction Expansion
  - Introducing an External Signal
  - Electron Beam Representation
- Numerical Results
  - Mode Competition in Coaxial Cavity Gyrotrons
  - Mode Cooperation in Harmonic Gyrotrons
  - Power Reflection Influence on Gyrotron Behavior
  - Nonstationary Operation of Gyro-BWOs
  - An Injection-Locked Gyro-BWO
- Conclusions

Introduction

Cyclotron Resonance

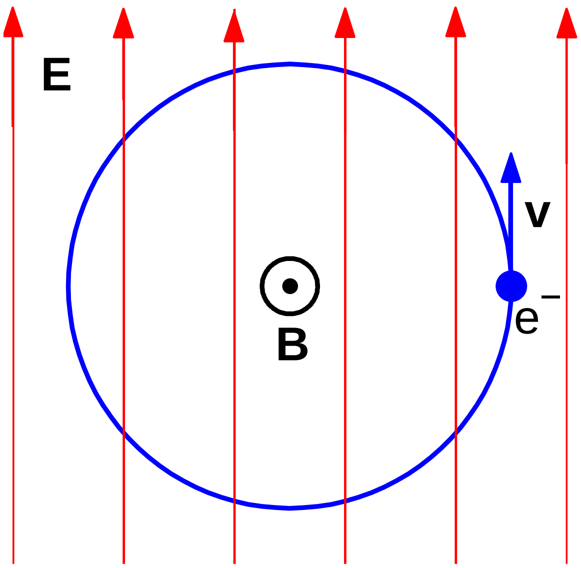

$$\boxed{\omega = s\Omega_c}$$

$$\Omega_c = \frac{e\mathbf{B}}{m\gamma}$$

$$\gamma = \frac{1}{\sqrt{1-\beta^2}}$$

$$\beta = \mathbf{v}/c$$

Introduction

Electron Bunching

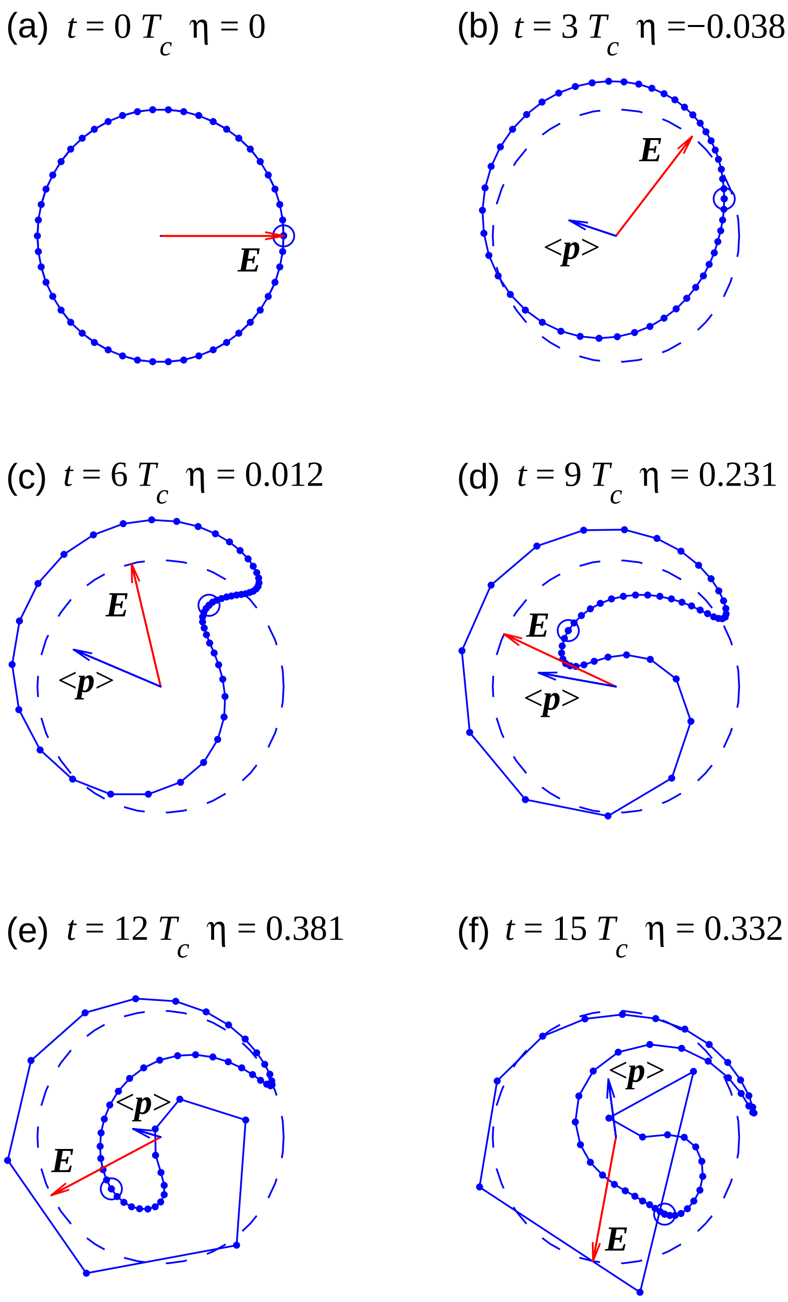

Frequency Mismatch

$$\Delta = \omega - s\Omega_c$$

Introduction

Gyrotron Scheme

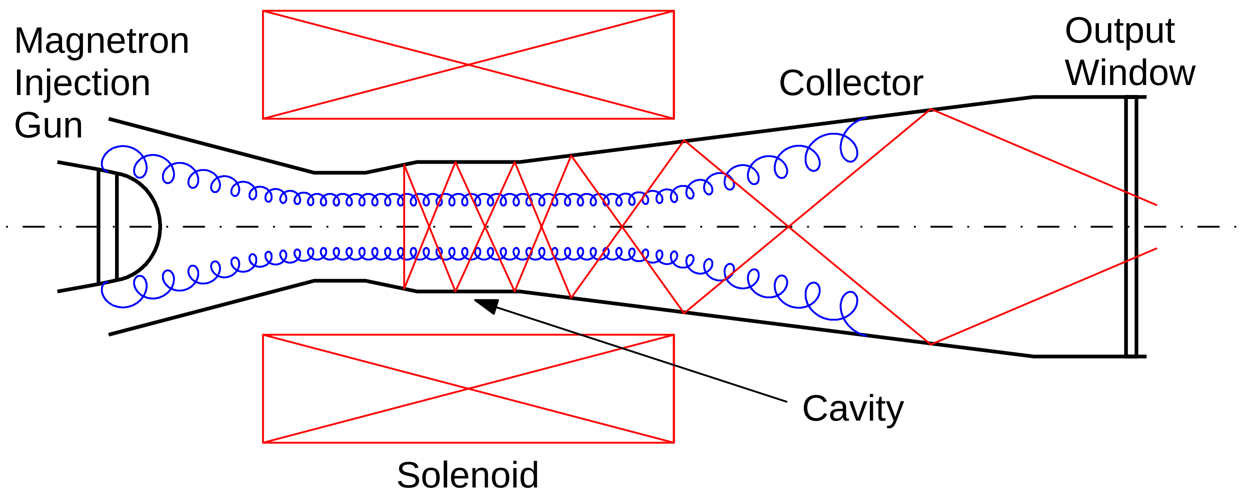

Introduction

Classification of Gyro-Devices

Schemes of O-type devices and corresponding gyro-devices

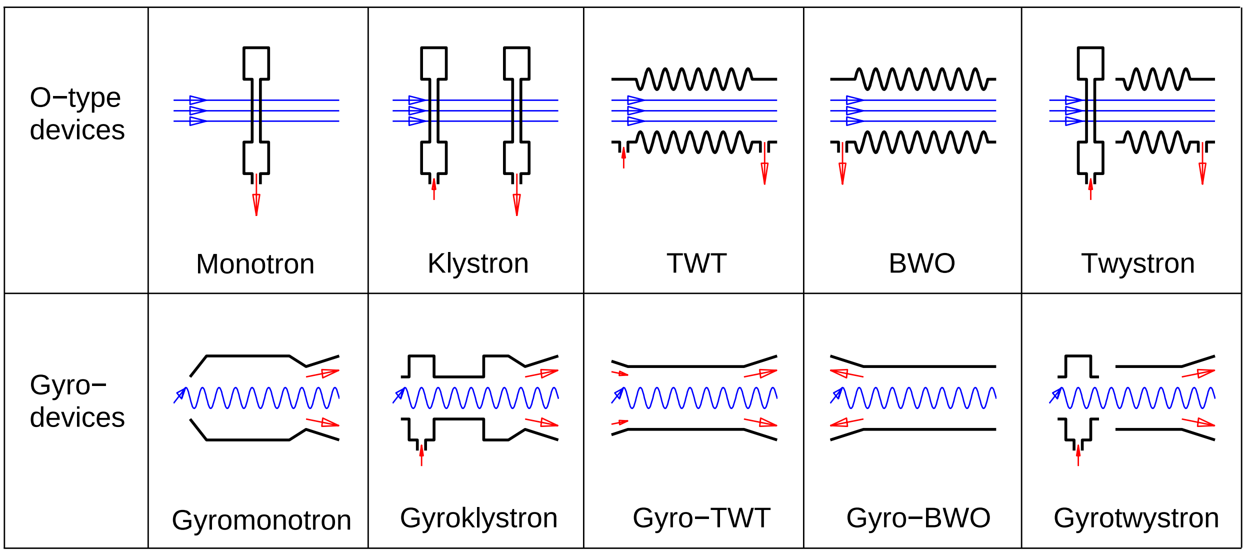

Introduction

Dispersion Relation for
a Gyrotron and a Gyro-BWO

$$\begin{cases} \omega = s\Omega_c + k_z v_z \\ \omega = \sqrt{\omega_c^2 + k_z^2 c^2} \end{cases}$$

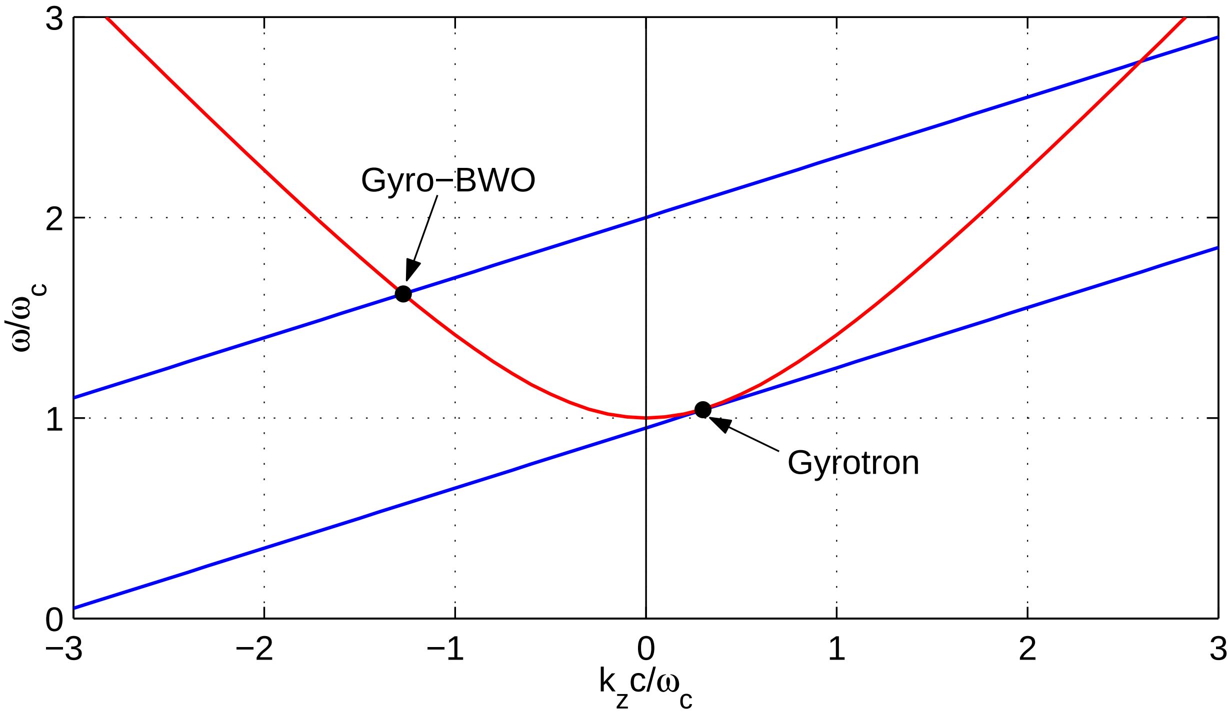

Theory

Eigenfunction Expansion

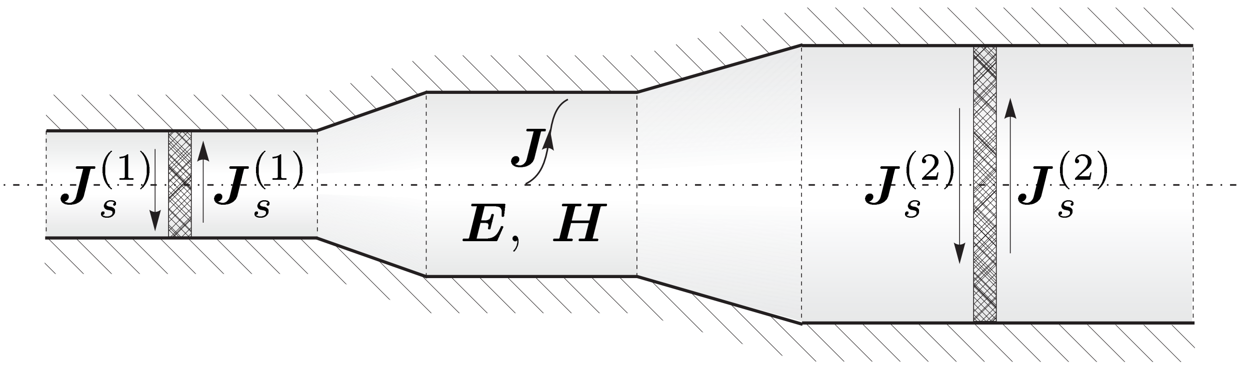

$$\boldsymbol{E} = \sum_n A_n\,\mathbf{E}_n + \sum_\alpha B_\alpha\,\mathbf{F}_\alpha$$

$$\boldsymbol{H} = \sum_n C_n\,\mathbf{H}_n + \sum_\lambda D_\lambda\,\mathbf{G}_\lambda$$

$$\boldsymbol{J} = \sum_n \tilde{A}_n\,\mathbf{E}_n + \sum_\alpha \tilde{B}_\alpha\,\mathbf{F}_\alpha$$

$$\nabla\cdot\mathbf{E}_n = 0 \quad ; \quad \nabla\times\mathbf{E}_n = k_n\,\mathbf{H}_n$$

$$\nabla\cdot\mathbf{H}_n = 0 \quad ; \quad \nabla\times\mathbf{H}_n = k_n\,\mathbf{E}_n$$

$$\nabla\times\mathbf{F}_\alpha = 0 \quad ; \quad \nabla f_\alpha = k_\alpha\,\mathbf{F}_\alpha$$

$$\nabla\times\mathbf{G}_\lambda = 0 \quad ; \quad \nabla g_\lambda = k_\lambda\,\mathbf{G}_\lambda$$

Theory

System of Equations for Matched Boundary Condition

$$\frac{1}{Z_0 c}\frac{\mathsf{d}}{\mathsf{d}t}A_n \quad - \; k_n\, C_n \quad = -\left[K_{nm}\right] I_m - \tilde{A}_n$$

$$\frac{1}{Z_0 c}\frac{\mathsf{d}}{\mathsf{d}t}B_\alpha \quad = -\left[\,\Lambda_{\alpha m}\right] I_m - \tilde{B}_\alpha$$

$$\frac{Z_0}{c}\frac{\mathsf{d}}{\mathsf{d}t}C_n \quad + \; k_n\, A_n \quad = \; 0$$

$$I_m = Y_m * V_m$$

$$V_m = \frac{1}{2}\left(\left[U\right] - \left[S\right]\right) * \left(\left[K_{nm}\right]^T a_n + \left[\,\Lambda_{\alpha m}\right]^T b_\alpha\right)$$

$$\frac{1}{Z_0 c}\frac{\mathsf{d}}{\mathsf{d}t}a_n \quad - \; k_n\, c_n \quad = -\tilde{A}_n$$

$$\frac{1}{Z_0 c}\frac{\mathsf{d}}{\mathsf{d}t}b_\alpha \quad = -\tilde{B}_\alpha$$

$$\frac{Z_0}{c}\frac{\mathsf{d}}{\mathsf{d}t}c_n \quad + \; k_n\, a_n \quad = \; 0$$

Theory

Introducing an External Signal $V^-(t)$ into the System

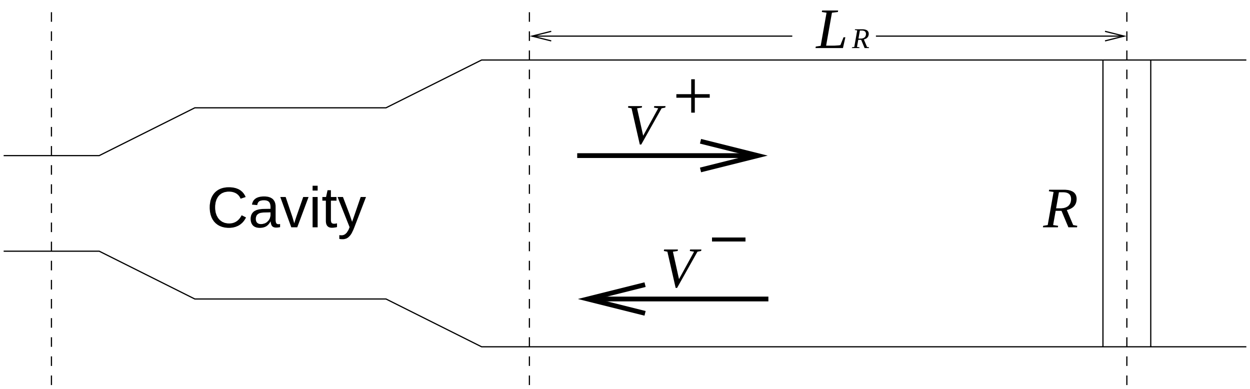

- Matched Operation: $V_m^-(t) = 0$
- Injection Signal: $V_m^-(t) = \mathsf{V}_m^{inj} \sin(\omega_m^{inj} t)$
- Reflection Signal: $V_m^-(t) = \left[R(t)\right] * V_m^+(t)$
  - Constant Reflection: $\mathrm{R}(\omega) = const$
  - Single Disk Dielectric Window

Theory

System of Equations for Mismatched Boundary Condition

$$\frac{1}{Z_0 c}\frac{\mathsf{d}}{\mathsf{d}t}A_n - k_n C_n = -\left[K_{nm}\right] I_m - \tilde{A}_n$$

$$\frac{1}{Z_0 c}\frac{\mathsf{d}}{\mathsf{d}t}B_\alpha = -\left[\Lambda_{\alpha m}\right] I_m - \tilde{B}_\alpha$$

$$\frac{Z_0}{c}\frac{\mathsf{d}}{\mathsf{d}t}C_n + k_n A_n = 0$$

$$I_m = I_m^+ - I_m^- \quad ; \quad I_m^\pm = Y_m * V_m^\pm$$

$$V_m^+ = V_m^- + \frac{1}{2}\left(\left[U\right] - \left[S\right]\right) * \left(\left[K_{nm}\right]^T a_n + \left[\Lambda_{\alpha m}\right]^T b_\alpha - 2V_m^-\right)$$

$$\frac{1}{Z_0 c}\frac{\mathsf{d}}{\mathsf{d}t}a_n - k_n c_n = -\tilde{A}_n$$

$$\frac{1}{Z_0 c}\frac{\mathsf{d}}{\mathsf{d}t}b_\alpha = -\tilde{B}_\alpha$$

$$\frac{Z_0}{c}\frac{\mathsf{d}}{\mathsf{d}t}c_n + k_n a_n = 0$$

Theory

Electron Beam Representation

$$\tilde{A}_n = \iiint_V \boldsymbol{J} \cdot \mathbf{E}_n \mathsf{d}V$$

$$\tilde{B}_\alpha = \iiint_V \boldsymbol{J} \cdot \mathbf{F}_\alpha \mathsf{d}V$$

$$\boldsymbol{J} = \sum_j \mathbf{v}_j q_j \delta(\mathbf{r} - \mathbf{r}_j)$$

$$\frac{\mathsf{d}}{\mathsf{d}t}\mathbf{p}_j = q_j \left[\boldsymbol{E} + \mathbf{v}_j \times (\mathbf{B} + \mu_0 \boldsymbol{H})\right]$$

$$\frac{\mathsf{d}}{\mathsf{d}t}\mathbf{r}_j = \mathbf{v}_j \quad \text{where} \quad \mathbf{p}_j = \gamma_j m_j \mathbf{v}_j$$

Numerical Results

Mode Competition in Coaxial Cavity Gyrotrons

Geometry of FZK coaxial gyrotron cavity

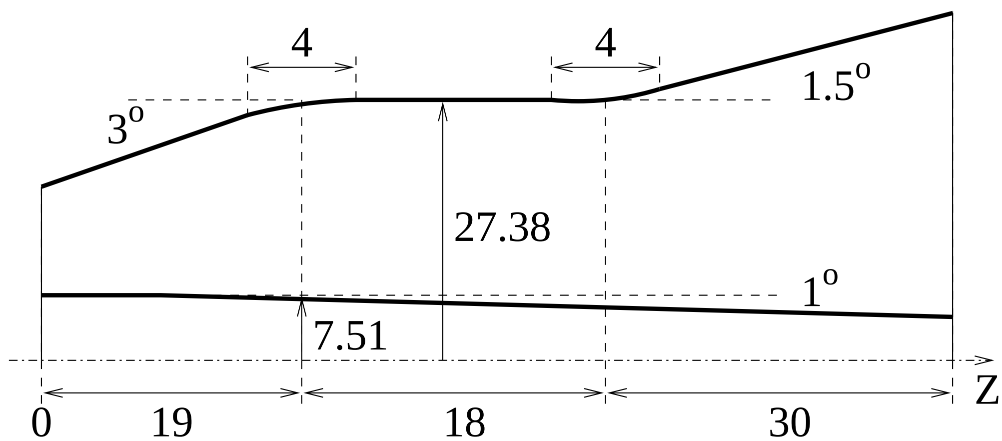

Parameters of FZK coaxial cavity gyrotron

Operating mode	$TE_{31,17}$
Operating frequency	$f_0 = 165$ GHz
Beam voltage	$V_b = 90$ kV
Beam current	$I_b = 50$ A
Beam radius	$r_b = 9.41$ mm
Pitch factor	$\alpha = 1.3$
Applied magnetic field	$B_0 = 6.65$ T

Numerical Results

Mode Competition in Coaxial Cavity Gyrotrons

Transverse field structure of the $\text{TE}_{31,17}$ mode

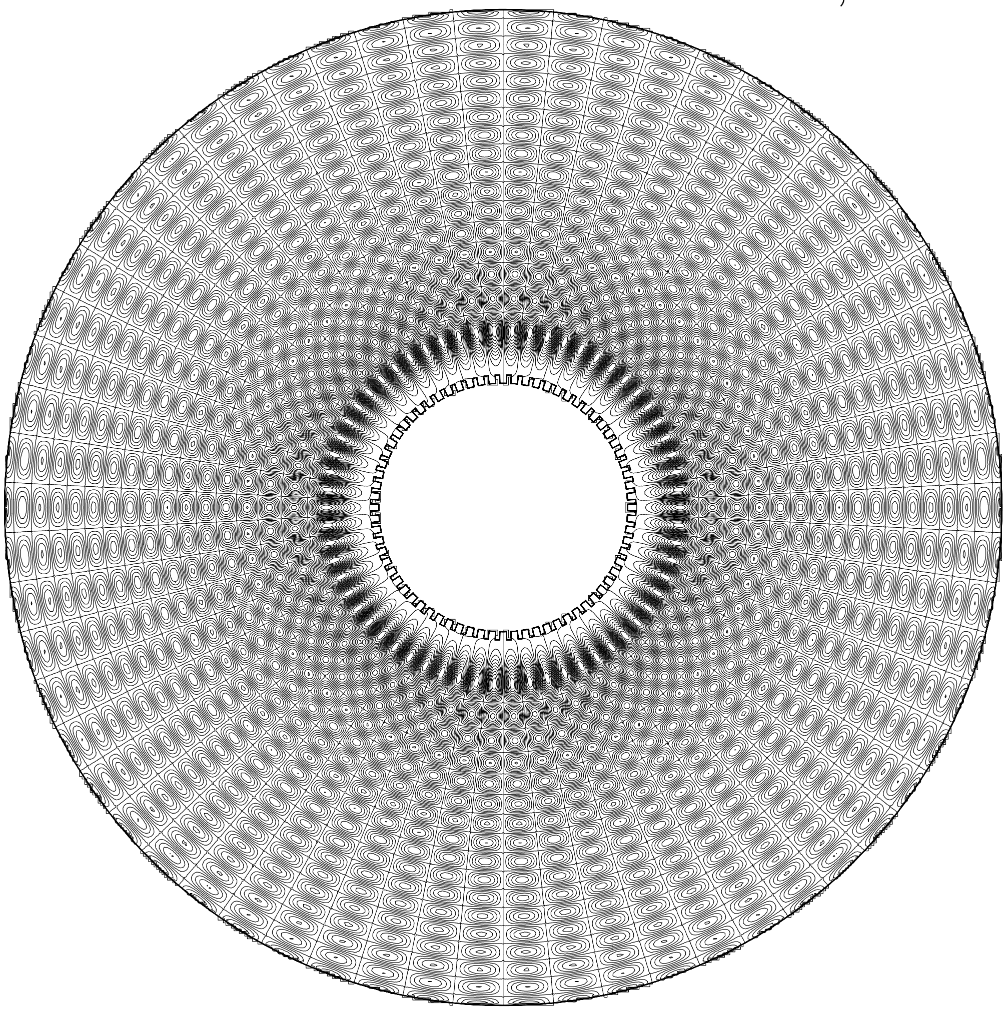

Corrugation depth	$d = 0.45$ mm
Corrugation width	$l = 0.35$ mm
Number of grooves	$N = 72$

Numerical Results

Mode Competition in Coaxial Cavity Gyrotrons

Mode competition in FZK coaxial cavity gyrotron

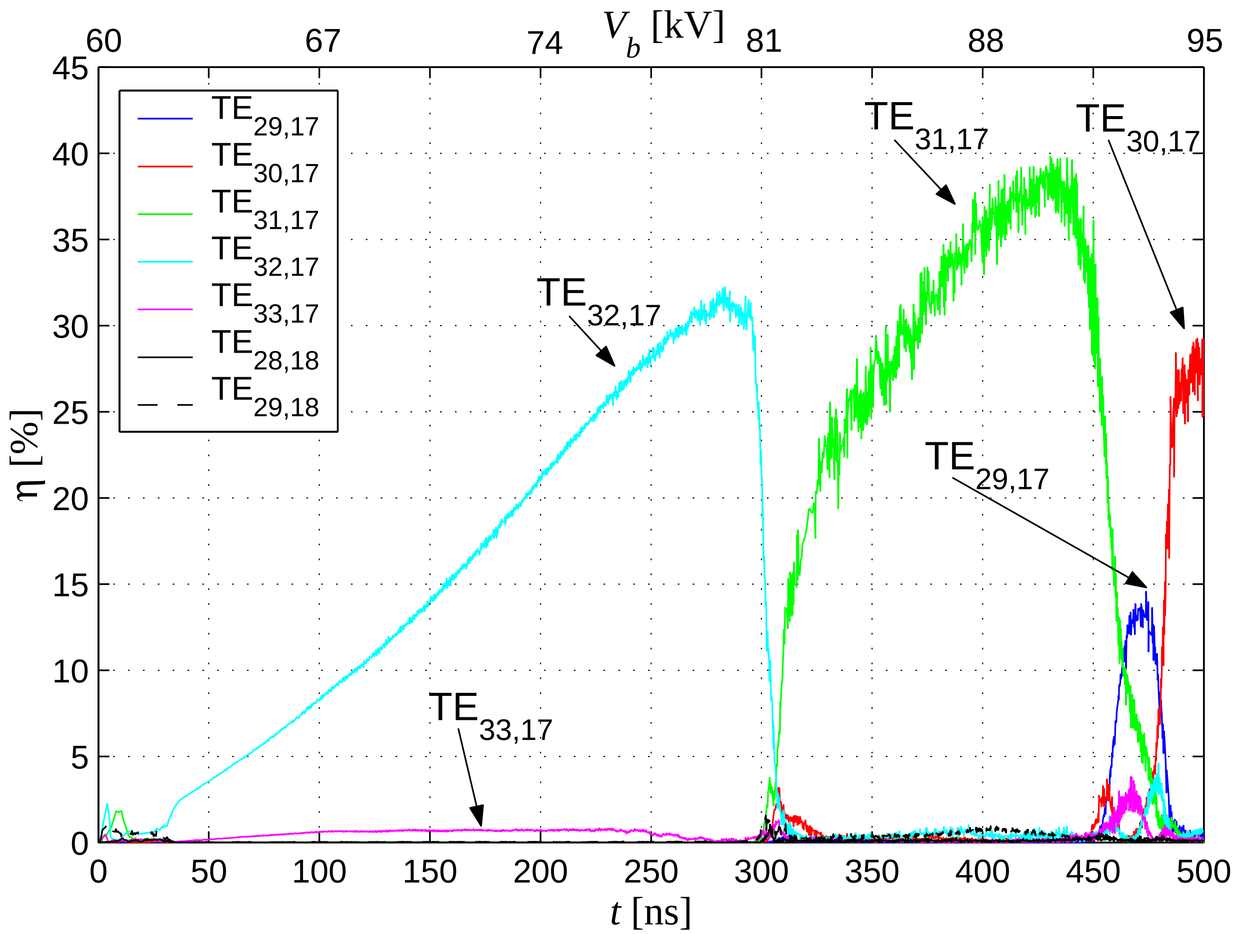

Numerical Results

Mode Cooperation in Harmonic Gyrotrons

Geometry of FUII harmonic gyrotron cavity

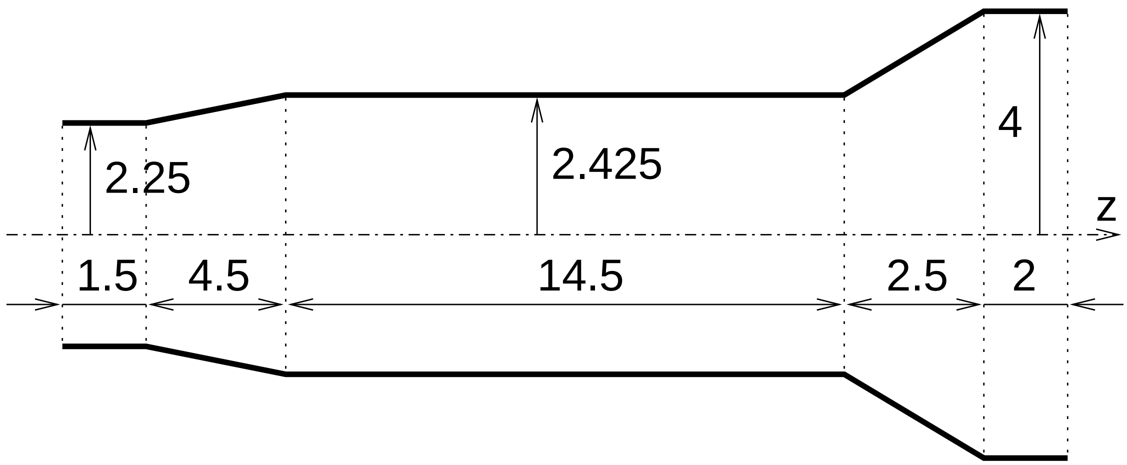

Parameters of FUII harmonic gyrotron

Operating mode	$TE_{2,6}$
Operating frequency	$f_0 = 384$ GHz
Beam current	$I_b = 1$ A
Beam voltage	$V_b = 40$ kV
Beam radius	$r_b = 1.25$ mm
Pitch factor	$\alpha = 1.5$
Applied magnetic field	$B_0 = 7.31$ T

Numerical Results

Mode Cooperation in Harmonic Gyrotrons

Dispersion diagram for the $TE_{2,3}$ and $TE_{2,6}$ modes

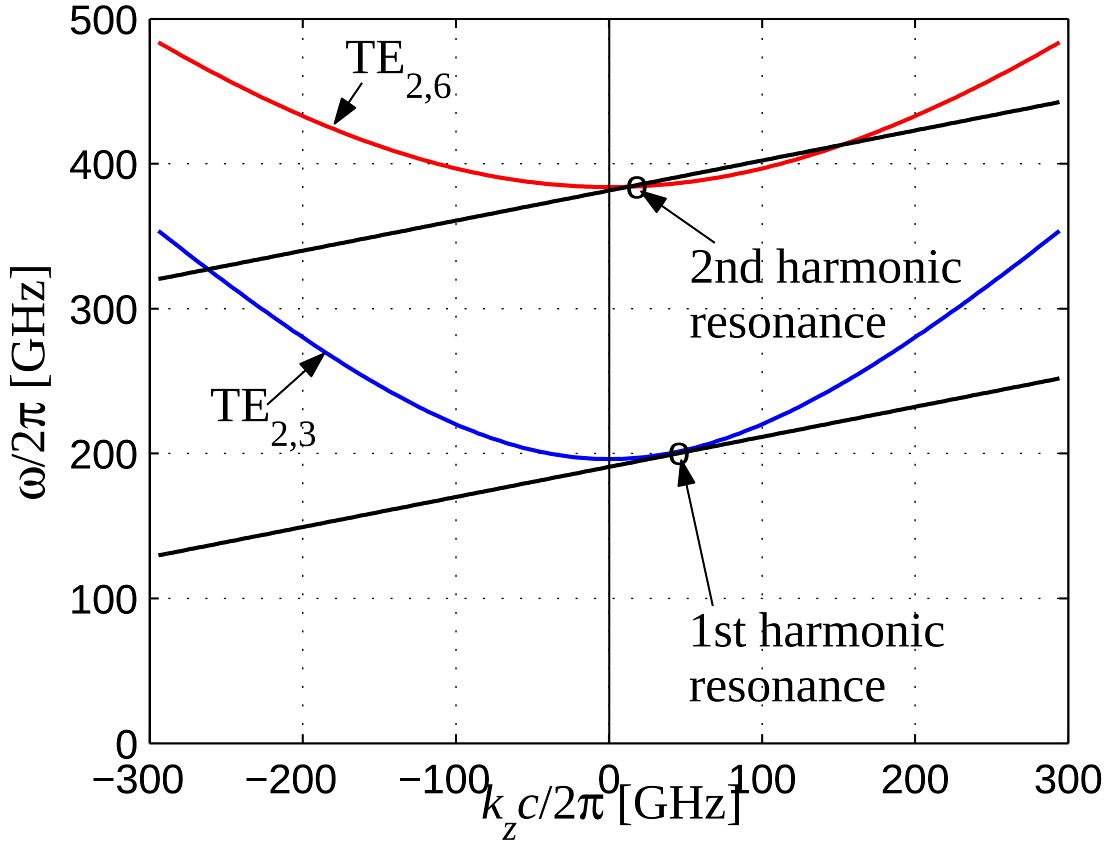

Numerical Results

Mode Cooperation in Harmonic Gyrotrons

Efficiency of the $TE_{2,3}$ and $TE_{2,6}$ modes versus time

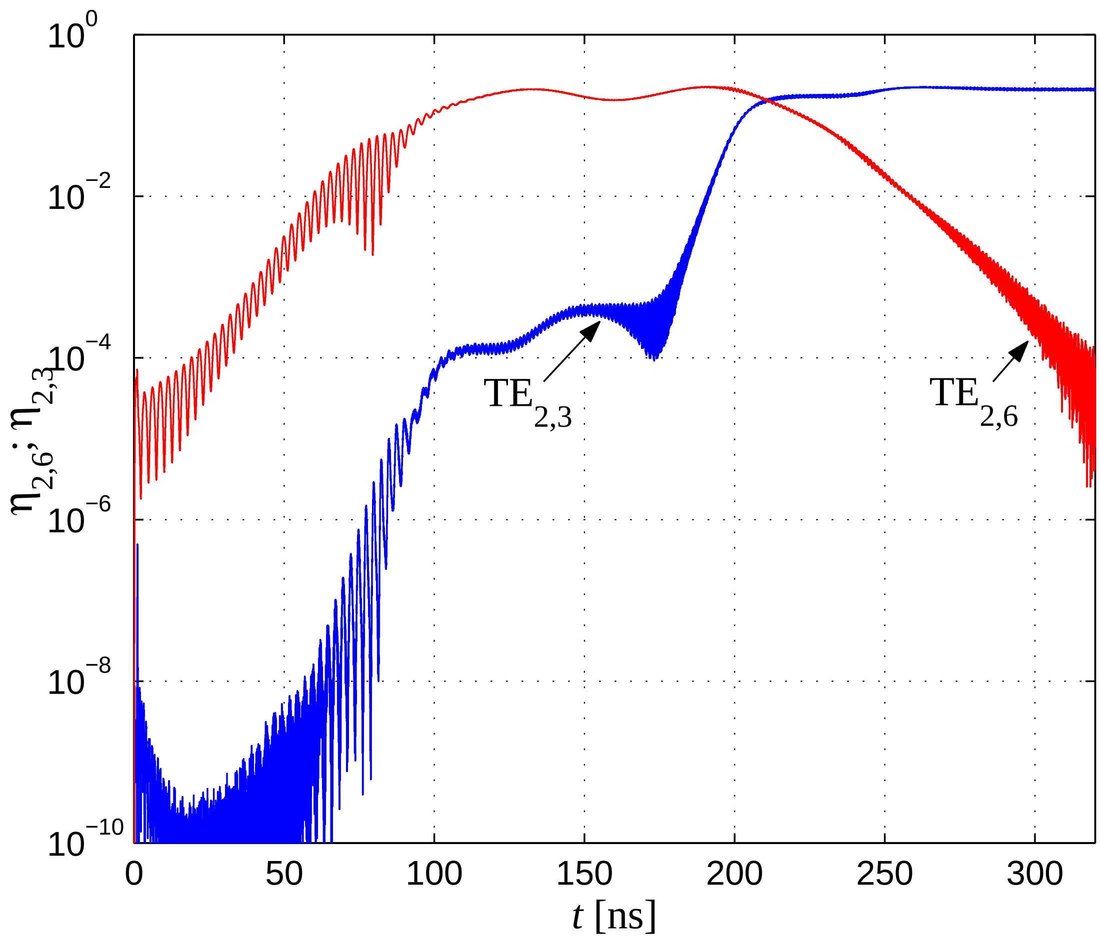

Numerical Results

Reflection Influence on Gyrotrons

Geometry of FZK gyrotron cavity

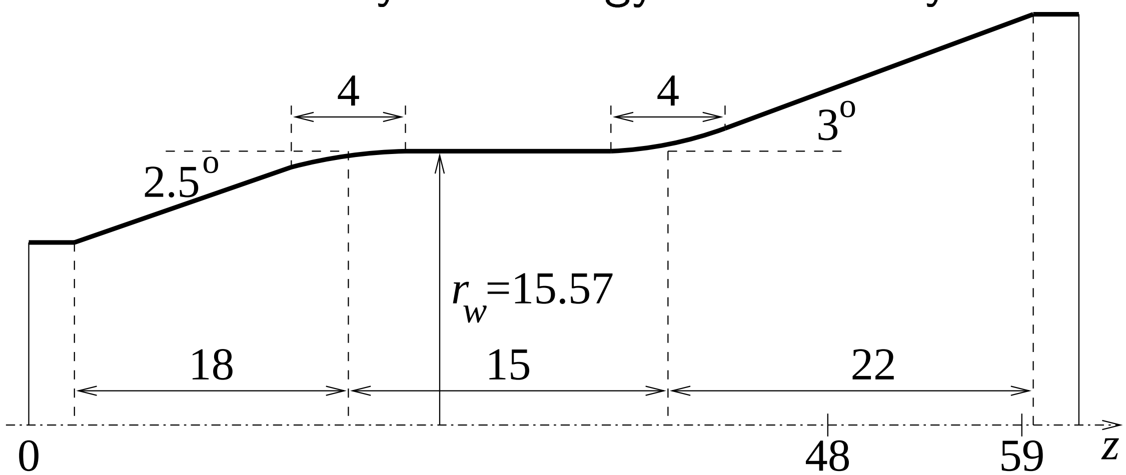

Parameters of FZK gyrotron

Operating mode	$TE_{22,6}$
Operating frequency	$f_0 = 140$ GHz
Beam voltage	$V_b = 80$ kV
Beam current	$I_b = 40$ A
Beam radius	$r_b = 8.1$ mm
Pitch factor	$\alpha = 1.4$
Applied magnetic field	$B_0 = 5.55$ T

Numerical Results

Reflection Influence on Gyrotrons

Output power and Spectra for $L_R = 1$ m

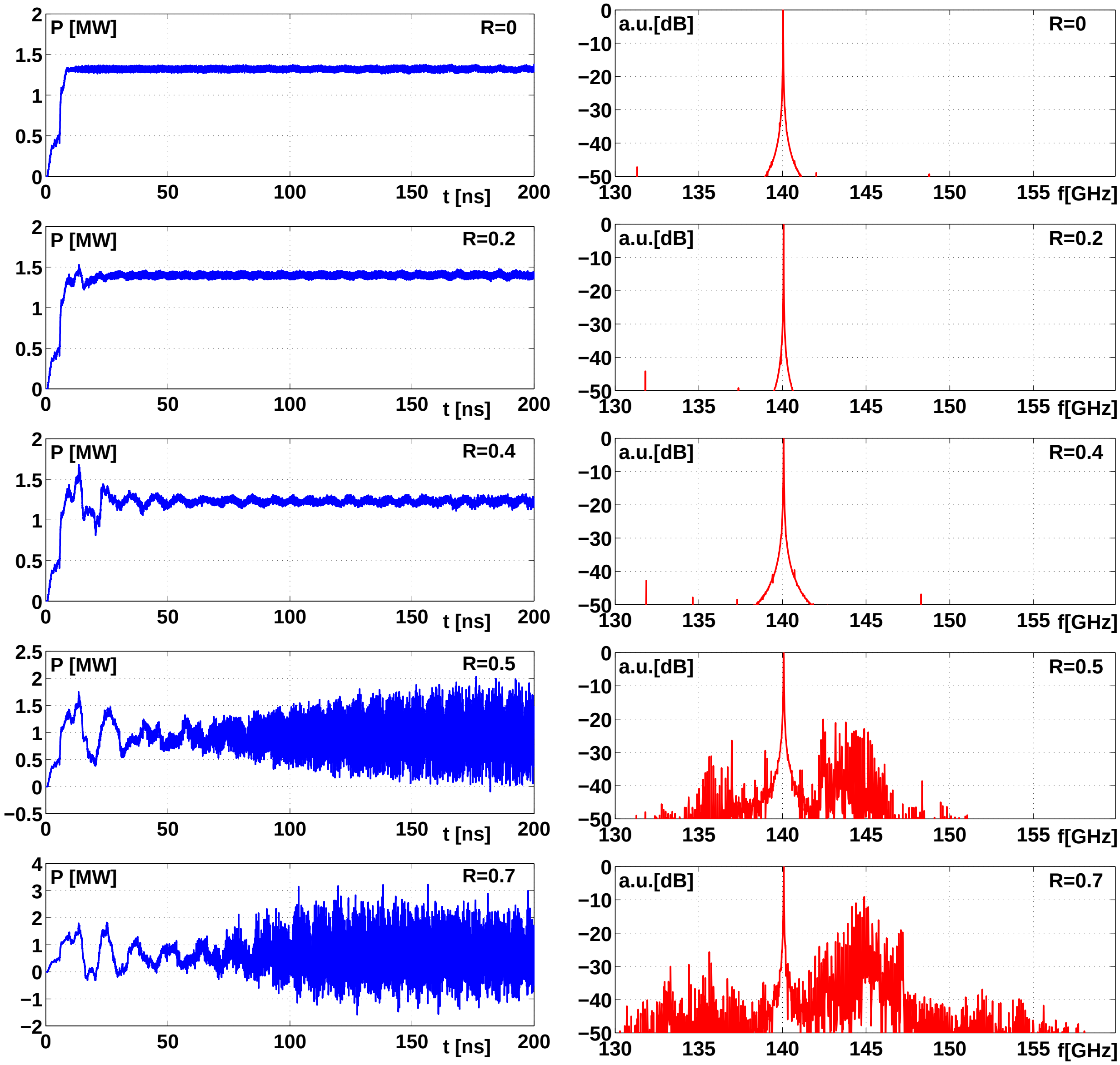

Numerical Results

Reflection Influence on Gyrotrons

Comparison between measured temperature increase and calculated output power

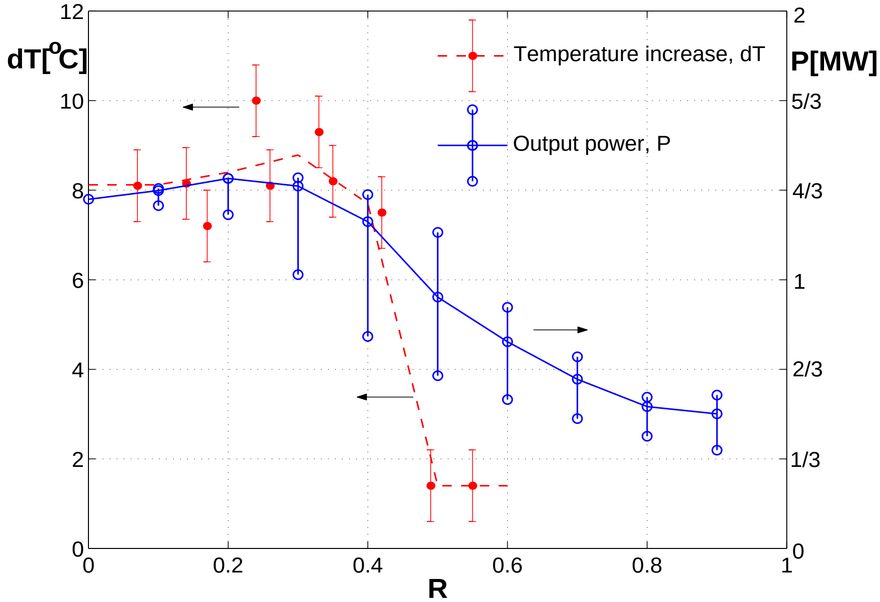

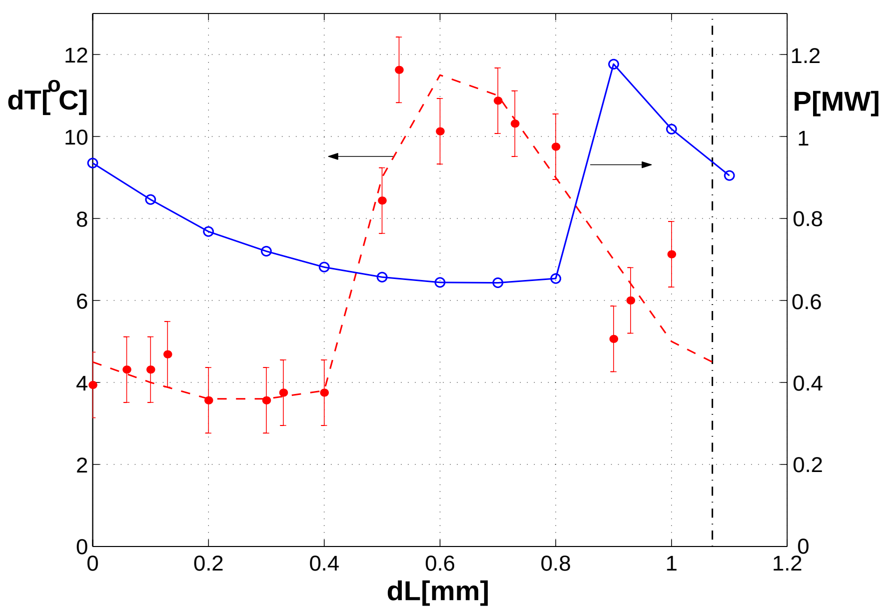

Numerical Results

Nonstationary Operation of Gyro-BWOs

Geometry of NTHU gyro-BWO structure

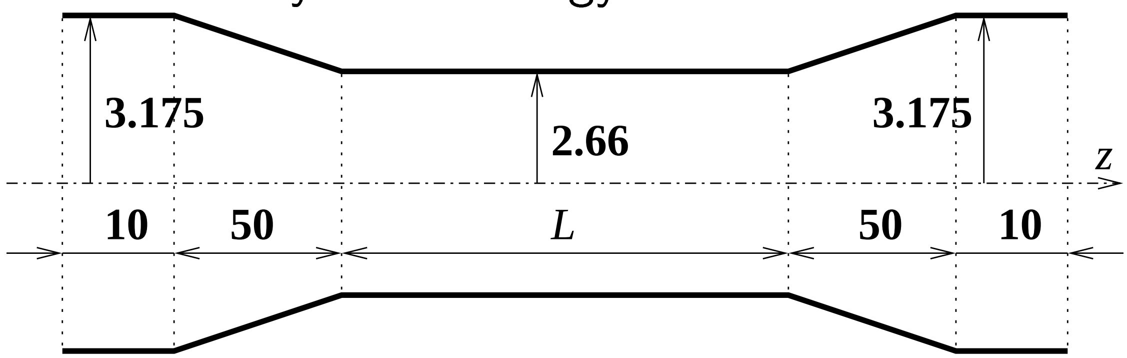

Parameters of NTHU gyro-BWO

Operating mode	$TE_{1,1}$
Operating frequency	$f_0 = 34$ GHz
Beam voltage	$V_b = 100$ kV
Beam current	$I_b = 4$ A
Beam radius	$r_b = 0.9$ mm
Pitch factor	$\alpha = 1$
Applied magnetic field	$B_0 = 1.459$ T

Numerical Results

Nonstationary Operation of Gyro-BWOs

Comparison of
measured ● and calculated ◇ efficiency
for $L = 100$ mm

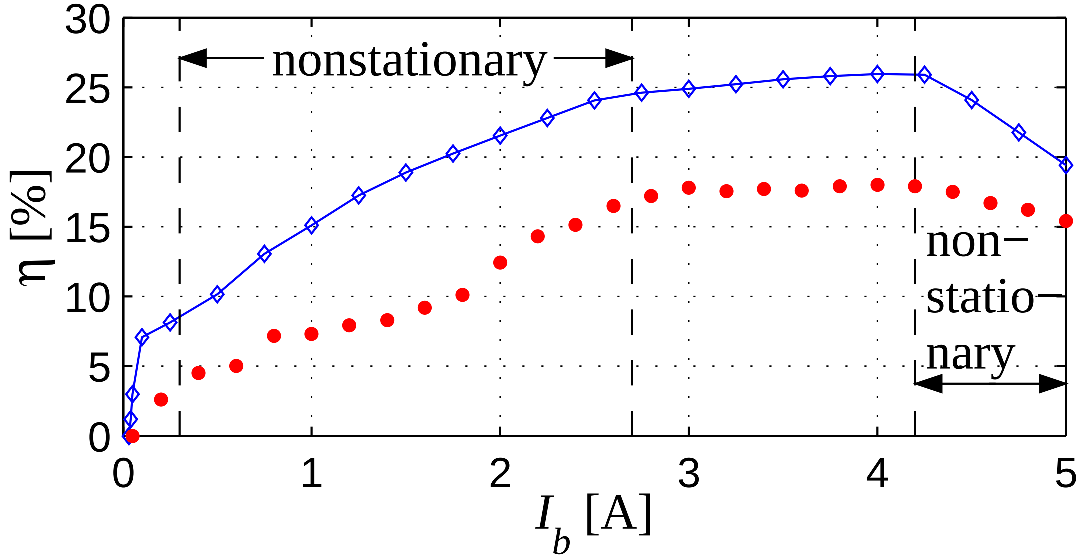

Efficiency versus time and Spectrum for $L = 100$ mm

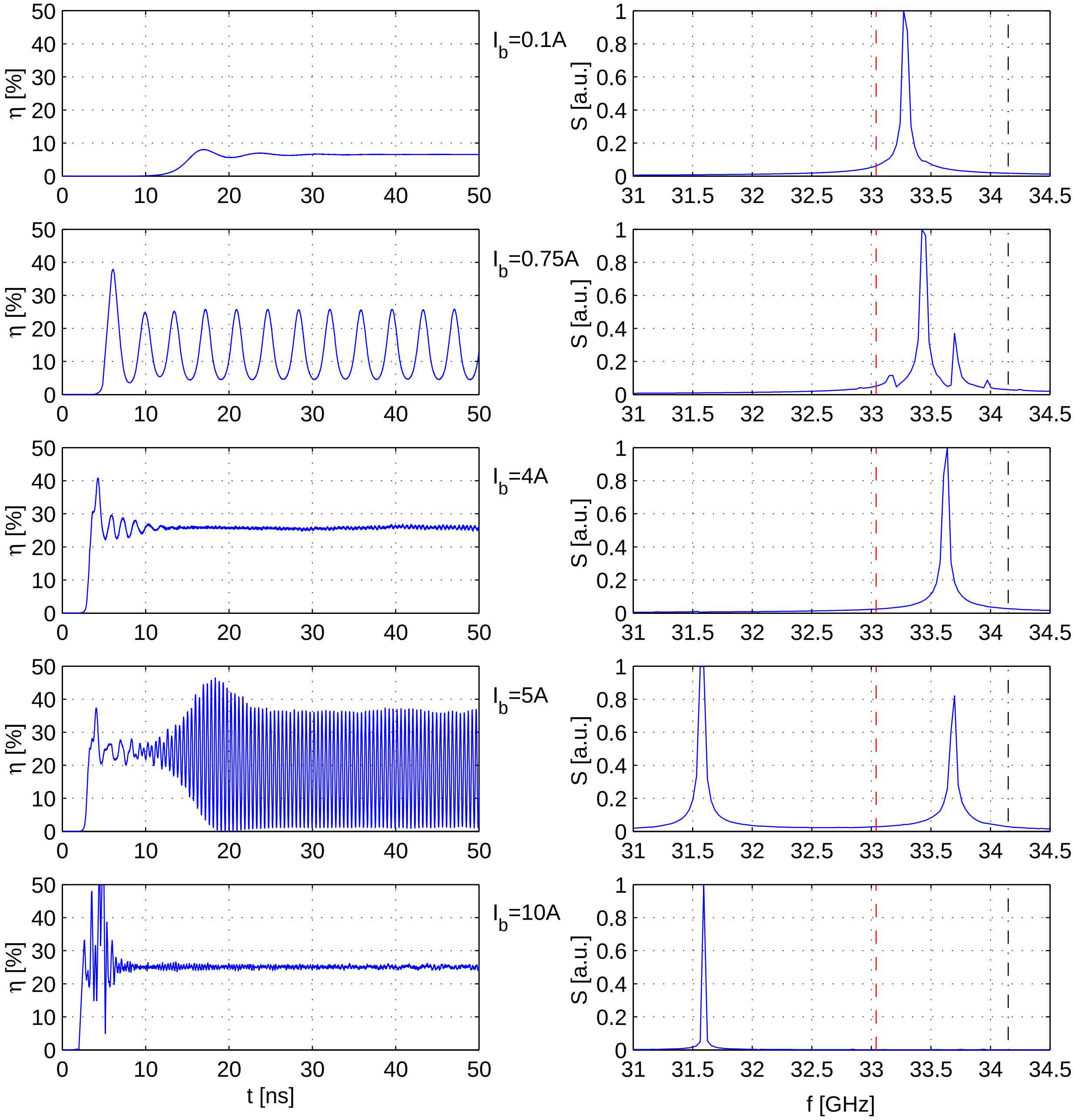

Numerical Results

Stability of Magnetic Tuning in Gyro-BWOs

Output power and frequency versus magnetic field for $L = 30$ mm

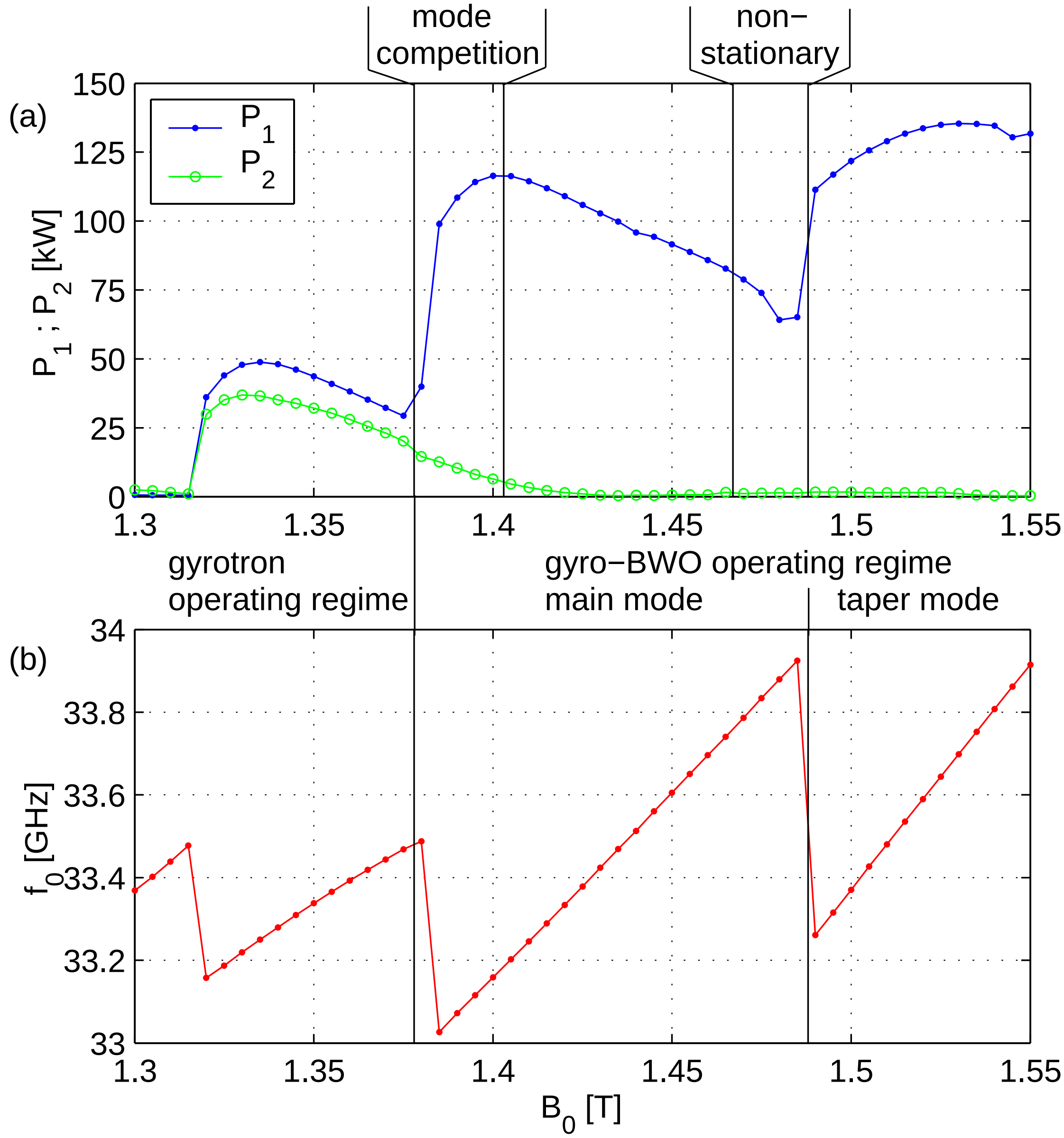

Numerical Results

Injection-Locked Operation of a Gyro-BWO

Locking bandwidth for different magnetic field

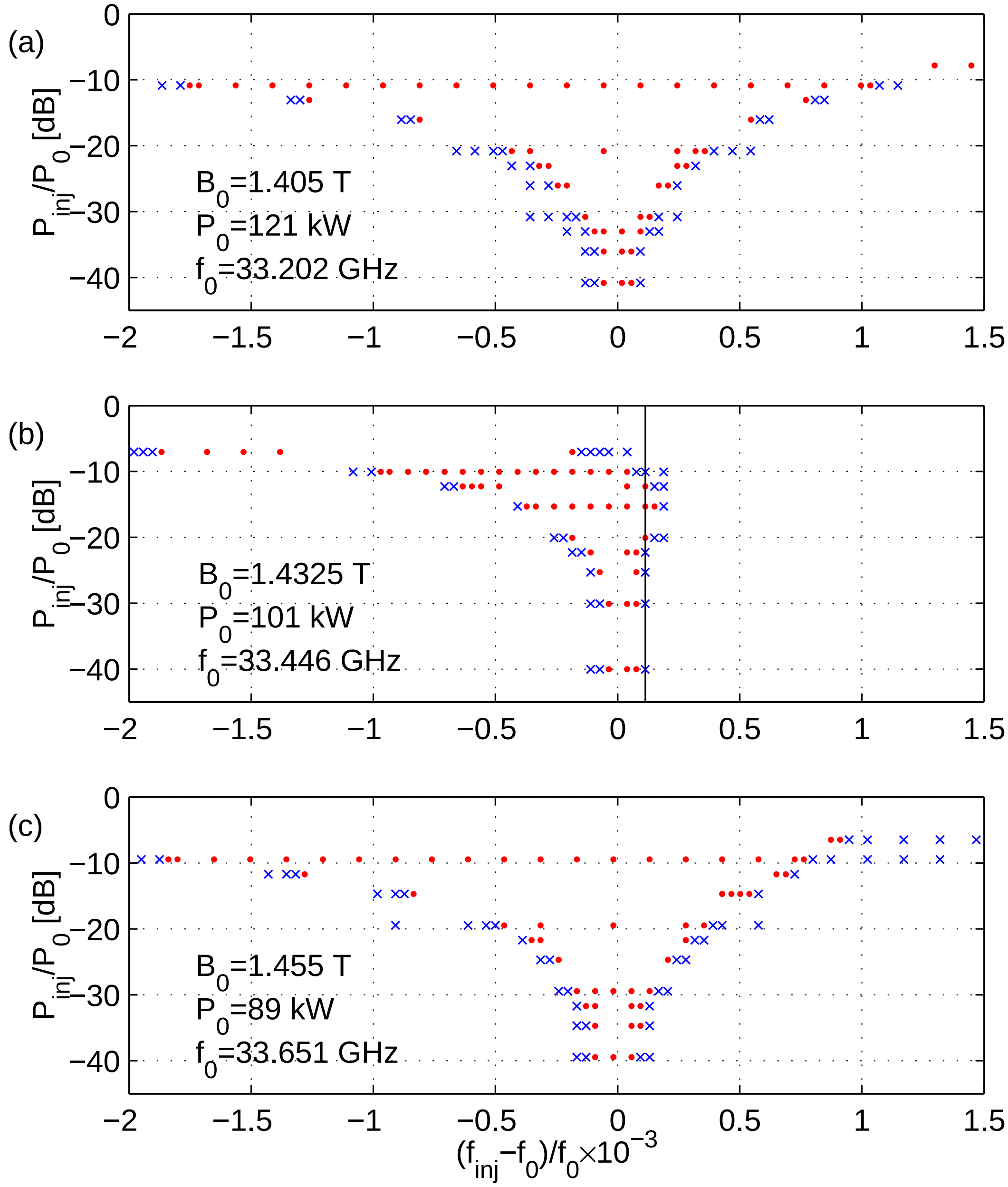

Conclusions

- A self-consistent time-dependent multimode analysis of gyro-oscillators has been developed.
- An interaction between the modes operating at the fundamental and/or higher harmonics of the cyclotron frequency has been investigated in both conventional and coaxial cavity gyrotrons.
- Reflection influence on gyrotron operation has been studied in terms of two models: constant reflection coefficient and single-disk dielectric window. Strong dependence on reflections has been found.
- Nonstationary phenomena in gyro-BWOs have been investigated, demonstrating an importance of time-dependent calculations for stability analysis.
- An injection-locked gyro-BWO has been studied, showing significant modifications of locking bandwidth when tuning the magnetic field.
- In general, the results of simulations are in a good agreement with available experimental results.